

Tree-based boosting with functional data

Xiaomeng Ju^{*}; Matías Salibián-Barrera

Department of Statistics
University of British Columbia

September 8, 2021

Abstract

In this article we propose a boosting algorithm for regression with functional explanatory variables and scalar responses. The algorithm uses decision trees constructed with multiple projections as the “base-learners”, which we call “functional multi-index trees”. We establish identifiability conditions for these trees and introduce two algorithms to compute them: one finds optimal projections over the entire tree, while the other one searches for a single optimal projection at each split.

We use numerical experiments to investigate the performance of our method and compare it with several linear and nonlinear regression estimators, including recently proposed nonparametric and semiparametric functional additive estimators. Simulation studies show that the proposed method is consistently among the top performers, whereas the performance of any competitor relative to others can vary substantially across different settings. In a real example, we apply our method to predict electricity demand using price curves and show that our estimator provides better predictions compared to its competitors, especially when one adjusts for seasonality.

Keywords: Boosting, Functional regression, Decision trees

^{*}Emails: xiaomeng.ju@stat.ubc.ca (Xiaomeng Ju), matias@stat.ubc.ca (Matías Salibián-Barrera)
This research is supported by Discovery Grant from the Natural Sciences and Engineering Research Council of Canada.

1 Introduction

Functional data consist of a sample of functional variables, which are often smooth functions measured on a discrete grid. In this article, we study regression problems with a functional covariate X and a scalar response Y , also called “scalar-on-function” regression, where the main goal is to estimate a function $F : X \rightarrow Y$ in order to make predictions for future observations of X .

Functional data are intrinsically infinite dimensional, and that poses challenges that vary with how the regression model is defined. Assuming that $X \in L^2(\mathcal{I})$ are square-integrable functions defined over an interval \mathcal{I} , the linear functional regression model is defined as $F(X) = \mu + \langle X, \beta \rangle$, where $\beta \in L^2(\mathcal{I})$ is the functional regression coefficient and $\langle X, \beta \rangle$ denotes the usual inner-product associated with the Hilbert space $L^2(\mathcal{I})$. Since β is infinite dimensional, its estimation requires some form of dimension reduction. A very common way of fitting this model is to represent β in some basis system (most often splines or functional principal components (FPCs)), and control its smoothness by regularizing the expansion, either through truncating the number of basis functions or by adding roughness penalties. A number of proposals in the literature explored different basis expansions and regularization strategies, for example Reiss and Ogden (2007), Zhao et al. (2012), Hall et al. (2007), and Cardot et al. (2003). For non-Gaussian responses, several authors studied the generalized functional linear model $g(F(X)) = \mu + \langle X, \beta \rangle$ for a known link function g , see, e.g. James (2002), Cardot and Sarda (2005), Müller et al. (2005), and Dou et al. (2012).

A well-specified linear model typically leads to a stable estimator associated with easy interpretation, however, a misspecified one can result in unreliable conclusions. Compared to linear models, nonparametric ones exhibit a higher degree of flexibility and have received recent attention in the functional context. We refer to Ferraty and Vieu (2006) and Ling and Vieu (2018) for general discussions on this topic. Various proposals adapted nonparametric regression in the finite dimensional case to functional data, many of which are based on kernels that require distances between pairs of explanatory variables. For functional data, natural measures of proximity involve notions of shape as those given by the similarities of derivatives or FPC scores (Shang, 2016). This suggests the use of semi-metrics as distance measures for many kernel-based functional regression estimators, including functional local-

constant/linear estimators (Ferraty and Vieu, 2002; Baíllo and Grané, 2009; Barrientos-Marin et al., 2010; Berlinet et al., 2011), functional k-nearest neighbours (Burba et al., 2009; Kudraszow and Vieu, 2013; Kara et al., 2017), functional recursive kernel estimator (Amiri et al., 2014), and Reproducing Kernel Hilbert Space (RKHS) methods (Preda, 2007; Avery et al., 2014). To avoid having to choose a semi-metric if several are available, Ferraty and Vieu (2009) and Febrero-Bande and González-Manteiga (2013) suggested to combine kernel estimators constructed with different semi-metrics.

It is well known that in finite dimensional settings nonparametric estimators suffer from the “curse of dimensionality” due to the sparseness of data in high-dimensional spaces. Similarly, the performance of kernel estimators for functional data is affected by sparsity in the infinite dimensional space, making it difficult to select a bandwidth when a data point has very few neighbours (Geenens et al., 2011; Mas et al., 2012). Exceptions derived from (generalized) additive models avoid this issue by imposing some structure on the target function. For example, Müller and Yao (2008) introduced a functional additive model with each component associated to a FPC score; Müller et al. (2013) and McLean et al. (2014) studied a continuous additive model $F(X) = \mu + \int G(X(t), t)dt$ and its generalized version where the additivity for both models occurs in the time domain. Their methods use splines to fit the smooth regression surface G with different regularization strategies.

Beyond linear and nonparametric models, there have been several developments towards semi-parametric regression for functional data, particularly in the direction of index-based models. Ling and Vieu (2020) summarized advances in this field in a recent survey. Ferraty et al. (2003) first proposed a functional single index model $F(X) = r(\langle X, \beta \rangle)$, where $r : \mathbb{R} \rightarrow \mathbb{R}$ is an unknown smooth function and $\beta \in L^2(\mathcal{I})$ is the functional regression coefficient. The computational and theoretical aspects of the proposal in Ferraty et al. (2003) were further explored by Ait-Saïdi et al. (2008), Ferraty et al. (2011), Jiang et al. (2011), and Goia and Vieu (2015).

To estimate more complex regression functions, some proposals studied multi-index models:

$$F(X) = r(\langle X, \alpha_1 \rangle, \dots, \langle X, \alpha_p \rangle), \tag{1}$$

where p is the number of indices and $r : \mathbb{R}^p \rightarrow \mathbb{R}$ is an unknown smooth function. Amato et al. (2006) proposed an extension of minimum average variance estimation to functional

data. Their method requires a p -dimensional kernel smoother to estimate r , which depends on a computationally expensive procedure to select p bandwidths and needs a large sample size to obtain a stable estimator when p is large. A few other proposals were derived from sliced inverse regression (Li, 1991), including functional sliced inverse regression (Ferré and Yao, 2003), functional k-means inverse regression (Wang et al., 2014), and functional sliced average variance estimation (Lian and Li, 2014). These methods avoid p -dimensional smoothing but require more restrictive assumptions on the distribution of X .

Another group of methods approximates F in (1) with a finite sum of single index terms:

$$F(X) \approx r_1(\langle X, \alpha_1 \rangle) + \dots + r_p(\langle X, \alpha_p \rangle). \quad (2)$$

This additive approximation is attractive since each component can be estimated by a single dimensional smoother that can be computed efficiently. Chen et al. (2011) and Ferraty et al. (2013) proposed iterative algorithms that estimate the r_j 's sequentially with kernel estimators, fitting one per iteration while keeping the previous ones fixed. For non-Gaussian responses, James and Silverman (2005) considered a generalized functional index model with a known link function and estimated the r_j 's with spline smoothers.

In this article, we propose a new way to estimate the regression function using a boosting algorithm. There exist other proposals that developed boosting-type algorithms for functional data, but they either apply to tasks different from ours (e.g. identifying the most predictive design points), or do not consider multi-index estimators (Ferraty et al., 2010; Tutz and Gertheiss, 2010; Fan et al., 2015; Ferraty and Vieu, 2009; Chen et al., 2011; Ferraty et al., 2013; Greven and Scheipl, 2017). Compared to these proposals, our approach fits more “closely” into a boosting framework by minimizing a loss function with a gradient descent-like procedure and applying regularization via shrinkage and early stopping.

Like gradient boosting, our algorithm constructs a regression estimator using a linear combination of “base learners”. The proposed algorithm can be thought of as fitting an approximation of the regression function

$$F(X) \approx r_1(\langle X, \beta_{1,1} \rangle, \dots, \langle X, \beta_{1,k} \rangle) + \dots + r_T(\langle X, \beta_{T,1} \rangle, \dots, \langle X, \beta_{T,K} \rangle), \quad (3)$$

where each of the T components $r_j(\langle X, \beta_{j,1} \rangle, \dots, \langle X, \beta_{j,K} \rangle)$ is characterized by K indices. Compared to (2), the approximation (3) enables modelling more complex structures of

the indices by including possible interactions. We fit each component with a tree-type base learner, which we call a “functional multi-index tree”, where the projection directions $\beta_{j,1}, \dots, \beta_{j,K}$ and $r_j : \mathbb{R}^K \rightarrow \mathbb{R}$ are calculated at the j -th boosting iteration.

The rest of this paper is organized as follows. In Section 2, we introduce in detail the functional regression model and our boosting algorithm, including identifiability conditions of functional multi-index trees and two algorithms to compute them. Section 3 reports the results of a simulation study comparing our method with existing alternatives. We discuss numerical results for a few representative settings and provide the complete set of results in the Appendix. A case study is presented in Section 4. Finally, Section 5 summarizes our findings and points out directions for future work.

2 Methodology

Consider a data set $(x_i, y_i), \dots, (x_n, y_n)$ with i.i.d. realizations of the pair (X, Y) , where X are predictor variables in some space \mathcal{X} , and Y is a scalar response. We are interested in estimating a function $F : \mathcal{X} \rightarrow Y$ in order to make predictions for future observations of X . Following Friedman (2001), we define the target function F as the minimizer of

$$F = \operatorname{argmin}_G E_{Y,X} L(Y, G(X)) \quad (4)$$

over the joint distribution of (X, Y) , where L is a pre-specified loss function such as the squared loss $L(a, b) = (a - b)^2$. Gradient boosting (Friedman, 2001) is a method to estimate F in (4) by constructing an approximate minimizer of the empirical risk:

$$\operatorname{argmin}_F \sum_{i=1}^n L(y_i, F(x_i)). \quad (5)$$

We view the objective in (5) as a function of the vector $(F(x_1), \dots, F(x_n))^T$. Similar to the gradient descent algorithm that sequentially adds to the current point the negative gradient vector of the objective function, gradient boosting adds to the current function estimate an approximation to the negative gradient vector. At the t -th iteration, the negative gradient vector $(u_{t,1}, \dots, u_{t,n})^T$ is computed at the point obtained from the previous iteration $(\hat{F}_{t-1}(x_1), \dots, \hat{F}_{t-1}(x_n))^T$:

$$u_{t,i} = -\frac{\partial L(y_i, b)}{\partial b} \Big|_{b=\hat{F}_{t-1}(x_i)}, \quad i = 1, \dots, n, \quad (6)$$

and is approximated using a base learner $\hat{h}_t : \mathcal{X} \rightarrow \mathbb{R}$ which we assume is characterized by parameters $\hat{\Theta}_t$ that are chosen to minimize

$$\sum_{i=1}^n (u_{t,i} - h_t(x_i; \Theta_t))^2,$$

over members h_t of a family of base learners (\mathcal{H}) and over Θ_t in the parameter space. We then calculate the step size

$$\hat{\alpha}_t = \operatorname{argmin}_{\alpha \in \mathbb{R}} \sum_{i=1}^n L(y_i, \hat{F}_{t-1}(x_i) + \alpha \hat{h}_t(x_i; \hat{\Theta}_t)).$$

and update

$$\hat{F}_t(x) = \hat{F}_{t-1} + \gamma \hat{\alpha}_t \hat{h}_t(x; \hat{\Theta}_t), \quad (7)$$

where $\gamma \in (0, 1)$ is a shrinkage parameter that controls the learning rate. The inclusion of γ is expected to reduce the impact of each base learner \hat{h}_t on \hat{F}_t by approximating more finely the search path, and as a result, improve the prediction accuracy (Telgarsky, 2013). This simple and effective strategy can be viewed as a form of regularization. Friedman (2001) showed empirically that a much lower prediction error can be achieved when $0 < \gamma \leq 0.1$.

Similar to what the gradient descent algorithm does, gradient boosting minimizes the training loss in a greedy fashion and may eventually overfit the training data at the expense of degraded generalization performance. To avoid this issue, boosting algorithms generally use an “early stopping” strategy that stops training when the performance on the validation set starts to deteriorate. We define an early stopping rule based on the performance on a validation set (\mathcal{V}) that follows the same model as the training set. Usually, the validation set is randomly selected from all available data and set aside from the training set. The early stopping time is defined as the iteration that achieves the lowest loss on \mathcal{V} :

$$T_{\text{stop}} = \operatorname{argmin}_{t=1, \dots, T_{\text{max}}} \sum_{i \in \mathcal{V}} L(y_i, \hat{F}_t(x_i)), \quad (8)$$

where T_{max} is the maximum number of iterations allowed in our algorithm. After training completes, the final boosting estimator is given by

$$\hat{F}_{T_{\text{stop}}}(x) = \hat{F}_0(x) + \sum_{t=1}^{T_{\text{stop}}} \gamma \hat{\alpha}_t \hat{h}_t(x; \hat{\Theta}_t),$$

where the initial function estimate is generally a constant defined as

$$\hat{F}_0(x) = \operatorname{argmin}_{a \in \mathbb{R}} \sum_{i=1}^n L(y_i, a).$$

Core to the performance of a boosting algorithm is the choice of base learners. In the functional context, for X in a Hilbert space \mathcal{L} (e.g. $L^2(\mathcal{I})$ the space of square-integrable functions) we will next introduce a flexible class of base learners which we call “functional multi-index trees”. They have the advantage of being capable of fitting functions of X that involve multiple projections and their possible interactions. Furthermore, they are scalable to large sample sizes and can easily incorporate additional real-valued explanatory variables.

2.1 Functional multi-index tree

When the explanatory variables are vectors in \mathbb{R}^d for some $d > 1$, decision trees are commonly used as base learners for gradient boosting, which select variables to make the best splits. Similarly for $X \in \mathcal{L}$, we “select” the optimal indices and use them to define the splits that partition the data.

Let $\beta_1, \dots, \beta_K \in \mathcal{L}$ be K functions which we view as projection directions. The inner-products $\langle x, \beta_1 \rangle, \dots, \langle x, \beta_K \rangle$ are corresponding indices projecting $x \in \mathcal{L}$ onto these directions. At the t -th iteration, we compute negative gradients $u_{t,i}$ as in (6) and define a functional multi-index tree $h(\langle \cdot, \beta_1 \rangle, \dots, \langle \cdot, \beta_K \rangle)$ as the solution to

$$\operatorname{argmin}_{h, \beta_1, \dots, \beta_K} \sum_{i=1}^n (u_{t,i} - h(\langle x_i, \beta_1 \rangle, \dots, \langle x_i, \beta_K \rangle))^2, \quad (9)$$

where $h : \mathbb{R}^K \rightarrow \mathbb{R}$ is a decision tree. In what follows, we will introduce two strategies to compute a functional multi-index tree: one chooses the optimal set of K indices over the entire tree, and the other finds a best single index at each split. We refer to the resulting trees as Type A and Type B trees, respectively.

2.1.1 Type A tree

The Type A tree takes a two-level approach where we estimate h at the inner level and search for the optimal $\hat{\beta}_1, \dots, \hat{\beta}_K$ at the outer level. It is easy to see this two-level structure if we re-state (9) as

$$\operatorname{argmin}_{\beta_1, \dots, \beta_K} \left\{ \operatorname{argmin}_h \sum_{i=1}^n (u_{t,i} - h(\langle x_i, \beta_1 \rangle, \dots, \langle x_i, \beta_K \rangle))^2 \right\}. \quad (10)$$

Given β_1, \dots, β_K , the inner level is simply fitting a usual decision tree using $\langle x_i, \beta_1 \rangle, \dots, \langle x_i, \beta_K \rangle$, $i = 1, \dots, n$ as predictors. At the outer level, we find β_1, \dots, β_K that minimize

$$\sum_{i=1}^n (u_{t,i} - \hat{h}(\langle x_i, \beta_1 \rangle, \dots, \langle x_i, \beta_K \rangle))^2. \quad (11)$$

If β_1, \dots, β_K are unconstrained, the solution to (10) is not unique. For example, for any decision tree h and non-zero real values b_1, \dots, b_k ,

$$h(\langle \cdot, \beta_1 \rangle, \dots, \langle \cdot, \beta_K \rangle) = \tilde{h}(\langle \cdot, b_1 \beta_1 \rangle, \dots, \langle \cdot, b_K \beta_K \rangle),$$

where the value at which the j -th input of h is split is multiplied by b_j in \tilde{h} . To avoid this issue, we introduce conditions under which h , β_1, \dots , and β_K are identifiable up to sign changes of each β_j :

Condition 1 $\|\beta_j\| = 1$, for $j = 1, \dots, K$.

Condition 2 Each index is chosen by at least one of the splits of a decision tree $h : \mathbb{R}^K \rightarrow \mathbb{R}$. For any set of indices $J \subset \{1, \dots, K\}$, there exist a $\delta > 0$ and $x_0 \in B(x_0, \delta) = \{x | x \in \mathcal{L}, \|x - x_0\| \leq \delta\}$, such that for $x \in B(x_0, \delta)$,

$$h(\langle L_1(x), \beta_1 \rangle, \dots, \langle L_j(x), \beta_j \rangle, \dots, \langle L_K(x), \beta_K \rangle) \quad (12)$$

is a non-constant function of x , where $L_j(x) = x$ if $j \in J$ and else $L_j(x) = x_0$, for $j = 1, \dots, K$.

The following result shows that these conditions are sufficient to generate a unique solution to (10) up to sign changes of each β_j . The proof of Theorem 1 is included in the Appendix.

Theorem 1 Suppose that Conditions 1 and 2 hold, then β_1, \dots, β_K are identifiable up to sign changes of each β_j . That means for any decision trees $h : \mathbb{R}^K \rightarrow \mathbb{R}$ and $\tilde{h} : \mathbb{R}^K \rightarrow \mathbb{R}$ if

$$h(\langle x, \beta_1 \rangle, \dots, \langle x, \beta_K \rangle) = \tilde{h}(\langle x, \eta_1 \rangle, \dots, \langle x, \eta_K \rangle) \quad (13)$$

hold for all $x \in \mathcal{L}$, then $\{\beta_1, \dots, \beta_K\} = \{(-1)^{l_1} \eta_1, \dots, (-1)^{l_K} \eta_K\}$ for some $l_1, \dots, l_K \in \{0, 1\}$, and $h = \tilde{h}$.

A convenient approach to find the solution of (10) is to approximate the optimal directions using a flexible basis (e.g. splines). Let $\{\psi_1, \dots, \psi_d\}$ be an orthonormal set in \mathcal{L} and write $\beta_j = \sum_{l=1}^d c_{j,l} \psi_l$. Then Condition 1 becomes $\|\mathbf{c}_j\|_2 = 1$ where $\|\cdot\|_2$ is the Euclidean norm and $\mathbf{c}_j = (c_{j,1}, \dots, c_{j,d})^T$ for $j = 1, \dots, K$. Condition 2 generally holds for functional multi-index trees except for very special situations, such as one of the indices being equal for all individuals.

With a slight abuse of notation, we define $\langle \cdot, \boldsymbol{\psi} \rangle = (\langle \cdot, \psi_1 \rangle, \dots, \langle \cdot, \psi_d \rangle)^T$ and write the objective in (10) as

$$\sum_{i=1}^n (u_{t,i} - h(\mathbf{c}_1^T \langle x_i, \boldsymbol{\psi} \rangle, \dots, \mathbf{c}_K^T \langle x_i, \boldsymbol{\psi} \rangle))^2. \quad (14)$$

To further simplify the computation to minimize (14) under the condition $\|\mathbf{c}_j\|_2 = 1$ for $j = 1, \dots, K$, we represent \mathbf{c}_j in a spherical coordinate system in order to obtain an optimization problem with simple box constraints.

Referring to Blumenson (1960), Cartesian coordinates \mathbf{c}_j and spherical coordinates $(r_j, \theta_{j,1}, \dots, \theta_{j,d-1})$ are connected through the following equations:

$$\begin{aligned} r_j &= \sqrt{\sum_{l=1}^d c_{j,l}^2} \\ c_{j,1} &= r_j \cos(\theta_{j,1}) \\ c_{j,l} &= r_j \cos(\theta_{j,l}) \prod_{k=1}^{l-1} \sin(\theta_{j,k}), \quad l = 2, \dots, d-1 \\ &\vdots \\ c_{j,d} &= r_j \prod_{k=1}^{d-1} \sin(\theta_{j,k}), \end{aligned}$$

where $r_j \in [0, \infty)$, $\theta_{j,1} \in [-\pi, \pi)$, and $\theta_{j,l} \in [0, \pi]$ for $l = 2, \dots, d-1$. As a result of this connection, we can transform \mathbf{c}_j to $(r_j, \theta_{j,1}, \dots, \theta_{j,d-1})$ and further reduce Condition 1 to $r_j = 1$. In addition, we restrict $\theta_{j,1} \in [-\pi/2, \pi/2)$, which is equivalent to $c_{j,1} > 0$. This restriction ensures that (14) has a single unique solution as opposed to multiple solutions that are unique up to sign changes.

Finally, we treat the objective of (14) as a function of $\boldsymbol{\theta}_j = (\theta_{j,1}, \dots, \theta_{j,d-1})^T$ and minimize it under conditions

$$\theta_{j,1} \in [-\pi/2, \pi/2), \theta_{j,2}, \dots, \theta_{j,d-1} \in [0, \pi]. \quad (15)$$

This can be achieved by applying generic gradient-free optimization algorithms that allow box constraints. Note that the objective function (14) may not be convex and therefore multiple starting points are recommended when performing the optimization (see Section 3.1 for details).

2.1.2 Type B tree

Unlike Type A trees which find K projection directions to minimize the prediction error of the whole tree, Type B trees adapt the CART algorithm (Breiman, 1984) to select an optimal direction at each split.

At each boosting iteration t , we start from $(x_1, u_{t,1}), \dots, (x_n, u_{t,n})$ and make the first split at the root node by finding the optimal split and the projection direction that solve

$$\operatorname{argmin}_{\beta} \left\{ \operatorname{argmin}_{g \in G_1} \sum_{i=1}^n (u_{t,i} - g(\langle x_i, \beta \rangle))^2 \right\}, \quad (16)$$

where G_1 denotes the class of single split trees, also called decision stumps. For any given β , the tree g partitions the data into two regions (nodes) where the dividing threshold is selected from $\langle x_1, \beta \rangle, \dots, \langle x_n, \beta \rangle$ to minimize the squared prediction error. To make predictions for data points in each region, the average responses of the training data in that region is used.

A Type B tree can be fitted by repeatedly solving (16) at each split. We can view (16) as a special case of fitting a Type A tree with $K = 1$ and depth $d = 1$, and apply the algorithm we introduced in Section 2.1.1. Having found the first split at the root node, we repeat the same process in each of the two resulted regions. This process is continued until the tree reaches its specified maximum depth.

This iterative optimization procedure is straightforward, but it can be computationally costly. There is also the concern of performing optimization at nodes that contain very few examples, for instance, nodes at deep levels of the tree, which may result in unstable estimation of β or even convergence failure of the optimization algorithm. To avoid these issues, we suggest an alternative approach to approximate the solution of (16).

Rather than solving (16) with respect to all possible β s at each split, we select β from a pool of randomly generated candidates. As we did for Type A trees, we expand β in the space of an orthonormal basis $\{\psi_1, \dots, \psi_d\}$ and let $\beta = \sum_{l=1}^d c_{0,l} \psi_l$. We randomly

generate a large pool of candidate \mathbf{c}_0 vectors denoted as $\mathcal{C}^{(t)} = \{\tilde{\mathbf{c}}_1^{(t)}, \dots, \tilde{\mathbf{c}}_P^{(t)}\}$, where each $\tilde{\mathbf{c}}_j^{(t)} \in \mathcal{C}^{(t)}$ is an independently sampled vector $\tilde{\mathbf{c}}_j^{(t)} = (\tilde{c}_{j,1}^{(t)}, \dots, \tilde{c}_{j,d}^{(t)})^T$ that satisfies $\|\tilde{\mathbf{c}}_j^{(t)}\|_2 = 1$ and $\tilde{c}_{j,1}^{(t)} > 0$. This ensures the candidate β s satisfy identifiability conditions $\|\tilde{\beta}_j\| = 1$ where $\tilde{\beta}_j = \sum_{l=1}^d \tilde{c}_{j,l}^{(t)} \psi_l$ for $j = 1, \dots, P$.

At each split, the coefficient vector of the projection direction is selected from $\mathcal{C}^{(t)}$. This corresponds to applying the CART algorithm to find a decision tree $h : \mathbb{R}^P \rightarrow \mathbb{R}$ that minimizes the squared error:

$$\operatorname{argmin}_h \sum_{i=1}^n \left(u_{t,i} - h \left((\tilde{\mathbf{c}}_1^{(t)})^T \langle x_i, \boldsymbol{\psi} \rangle, \dots, (\tilde{\mathbf{c}}_P^{(t)})^T \langle x_i, \boldsymbol{\psi} \rangle \right) \right)^2, \quad (17)$$

where $(\tilde{\mathbf{c}}_1^{(t)})^T \langle x_i, \boldsymbol{\psi} \rangle, \dots, (\tilde{\mathbf{c}}_P^{(t)})^T \langle x_i, \boldsymbol{\psi} \rangle$ are the explanatory variables and $u_{t,i}$ is the response for the i -th individual. In order to reduce overfitting, we use different pools $\mathcal{C}^{(t)}$ randomly chosen at each boosting iteration. This is expected to introduce randomness to the algorithm and allow more directions to be considered.

We point out that Type B trees cannot fully replace Type A trees as either type is preferred in different situations. If the target function is complex and requires a base learner with high complexity to achieve satisfactory prediction accuracy, we suggest using Type B trees, taking advantage of its fast computation and flexible structure. On the other hand, when the target function is simple, parsimonious base learners (e.g. Type A trees with few indices) are often preferred to prevent overfitting. Note that both Type A and B trees can easily include real-valued explanatory variables $\mathbf{v}_i \in \mathbb{R}^q$ by replacing $h(\langle x_i, \beta_1 \rangle, \dots, \langle x_i, \beta_K \rangle)$ in (9) with $h(\langle x_i, \beta_1 \rangle, \dots, \langle x_i, \beta_K \rangle, \mathbf{v}_i)$. More specifically, (14) becomes

$$\sum_{i=1}^n (u_{t,i} - h(\mathbf{c}_1^T \langle x_i, \boldsymbol{\psi} \rangle, \dots, \mathbf{c}_K^T \langle x_i, \boldsymbol{\psi} \rangle, \mathbf{v}_i))^2, \quad (18)$$

for Type A trees, and (17) becomes

$$\operatorname{argmin}_h \sum_{i=1}^n \left(u_{t,i} - h \left((\tilde{\mathbf{c}}_1^{(t)})^T \langle x_i, \boldsymbol{\psi} \rangle, \dots, (\tilde{\mathbf{c}}_P^{(t)})^T \langle x_i, \boldsymbol{\psi} \rangle, \mathbf{v}_i \right) \right)^2 \quad (19)$$

for Type B trees. This extension allows our method to fit partial-functional regression models with mixed-type predictors. In Section 4, we will introduce an example that illustrates the usage of our method in a partial-functional setting.

3 Simulation

To assess the numerical performance of our proposed method, we conducted a simulation study comparing it with alternative functional regression methods in the literature.

We generated data sets $D = \{(x_i, y_i), i = 1, \dots, N\}$, consisting of a predictor $x_i \in L^2(\mathcal{I})$ and a scalar response y_i that follow the model:

$$y_i = r(x_i) + \rho\epsilon_i, \quad (20)$$

where the errors ϵ_i are i.i.d $N(0, 1)$, r is the regression function, and $\rho > 0$ is a constant that controls the signal-to-noise ratio (SNR):

$$\text{SNR} = \frac{\text{Var}(r(X))}{\text{Var}(\rho\epsilon)}.$$

To sample the functional predictors x_i , we considered two models adopted from Ferraty et al. (2013) and Boente and Salibian-Barrera (2021) respectively:

- Model 1 (M_1):

$$x_i(t) = a_i + b_i t^2 + c_i \exp(t) + \sin(d_i t),$$

where $t \in [-1, 1]$, $a_i, b_i \sim \mathcal{U}(0, 1)$, $c_i \sim \mathcal{U}(-1, 1)$, and $d_i \sim \mathcal{U}(-2\pi, 2\pi)$; and

- Model 2 (M_2):

$$x_i(t) = \mu(t) + \sum_{p=1}^4 \sqrt{\lambda_p} \xi_{ij} \phi_j(t),$$

where $t \in [0, 1]$, $\mu(t) = 2 \sin(t\pi) \exp(1-t)$, $\lambda_1 = 0.8$, $\lambda_2 = 0.3$, $\lambda_3 = 0.2$, and $\lambda_4 = 0.1$, $\xi_{ij} \sim N(0, 1)$, and ϕ_j 's are the first four eigenfunctions of the ‘‘Mattern’’ covariance function $\gamma(s, t)$ with parameters $\rho = 3$, $\sigma = 1$, $\nu = 1/3$:

$$\gamma(s, t) = C \left(\frac{\sqrt{2\nu}|s-t|}{\rho} \right), \quad C(u) = \frac{\sigma^2 2^{1-\nu}}{\Gamma(\nu)} u^\nu K_\nu(u),$$

where $\Gamma(\cdot)$ is the Gamma function and K_ν is the modified Bessel function of the second kind.

For each subject i , we evaluated x_i on a dense grid t_1, \dots, t_{100} in $\mathcal{I} = [-1, 1]$ for M_1 and $\mathcal{I} = [0, 1]$ for M_2 . Figure 1 shows an example of 10 randomly sampled x_i 's generated from M_1 (left panel) and M_2 (right panel).

We considered five regression functions:

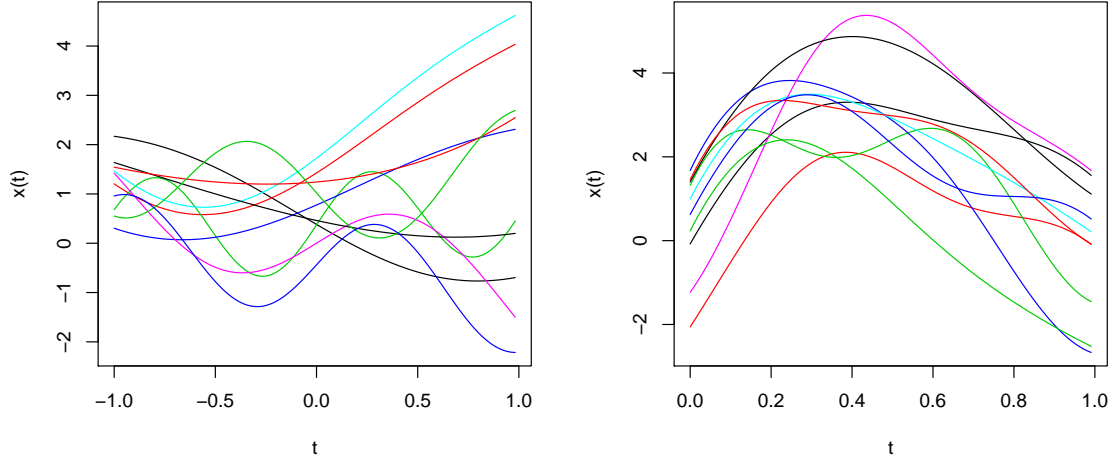


Figure 1: Ten random samples generated from Model 1 (left panel) and Model 2 (right panel).

- $r_1(X) = \left(\int_{\mathcal{I}} (X(t) - \mu(t))(\phi_1(t) + \phi_2(t)) dt \right)^{1/3}$, where the first two FPCs (ϕ_1 and ϕ_2) and mean (μ) for M_1 were calculated using a large sample of $x_i, i = 1, \dots, 3000$, while for M_2 their true values were used,
- $r_2(X) = 5 \exp \left(-\frac{1}{2} \left| \int_{\mathcal{I}} x(t) \log(|x(t)|) dt \right| \right)$,
- $r_3(X) = 5 \text{logistic} \left(2 \int_{\mathcal{I}} X(t)^2 \sin(2\pi t) dt \right)$, where $\text{logistic}(u) = 1/(1 + \exp(-u))$, and
- $r_4(X) = 5 \left(\sqrt{\left| \int_{\mathcal{I}_1} \cos(2\pi t^2) X(t) dt \right|} + \sqrt{\left| \int_{\mathcal{I}_2} \sin(X(t)) dt \right|} \right)$, where $\mathcal{I}_1 = [-1, 0]$ and $\mathcal{I}_2 = (0, 1]$ for M_1 , and $\mathcal{I}_1 = [0, 0.5]$ and $\mathcal{I}_2 = (0.5, 1]$ for M_2 .

These regression functions were selected to represent a single-index model (r_1) and other nonlinear models (r_2, r_3 , and r_4). To control the level of noise, we considered SNR = 5 and 20 as high and low noise levels and denoted them as S_1 and S_2 , For each combination of the predictor model (M), regression function (r), and noise level (S), we generated i.i.d. samples $(x_i, y_i), \dots, (x_N, y_N)$ of size $N = 1600$. The dataset was randomly partitioned into a training set, a validation set, and a test set of size 400, 200, and 1000 respectively. In total, we simulated data from 16 settings, each defined as a combination (M, r, S) from the set $\{M_1, M_2\} \times \{r_1, \dots, r_4\} \times \{S_1, S_2\}$.

3.1 Implementation details

For each setting, we used 100 independently generated datasets and compared the performance of the following estimators:

- **FLM1**: functional linear regression with cubic B-splines (Hastie and Mallows, 1993),
- **FLM2**: functional linear regression with FPC scores (Cardot et al., 1999),
- **FAM**: functional additive models (Müller and Yao, 2008),
- **FAME**: functional adaptive model estimation (James and Silverman, 2005),
- **FPPR**: functional projection pursuit regression (Ferraty et al., 2013),
- **FGAM**: functional generalized additive models (McLean et al., 2014),
- **TFBoost(A,K)**: tree-based functional boosting with Type A trees, where each tree is specified with $K = 1, 2,$ or 3 indices, and
- **TFBoost(B)**: tree-based functional boosting with Type B trees.

FLM1 and **FLM2** are classical functional regression methods for linear models, and they use different bases to estimate the regression coefficients. For **FLM1**, we used cubic B-splines with 7 basis functions (3 evenly spaced interior knots), which was found to work generally well compared to using less or more interior knots. We penalized the second derivative of the coefficient and selected the penalization parameter to minimize the mean-squared-prediction-error (MSPE) on the validation set. For **FLM2**, we used the top 4 FPCs required to explain 99% of the variance.

FAM constructs an additive estimator using FPC scores as predictors. We modified its implementation in the `fdapace` package (Carroll et al., 2021) to select the number of FPC scores that minimizes the MSPE on the validation set.

FAME estimates an extension of generalized additive models (GAM) to functional predictors. We used the code shared by the authors of James and Silverman (2005) and fitted the model using a Gaussian link function. **FPPR** follows the principle of projection pursuit regression and assumes an additive decomposition with each component being a functional single index model (FSIM). We implemented **FPPR** using the code to fit a single additive component shared by the authors of Ferraty et al. (2013) and built an estimator by adding

multiple functional single index estimators. Similarly to what was done with `FLM1`, for `FPPR` and `FAME` we used cubic B-splines with 7 functions (3 evenly spaced interior knots) as the basis. For both methods, we selected the number of additive components between 1 and 15 to minimize the MSPE on the validation set. In our simulation settings, the performance of `FAME` and `FPPR` rarely improved beyond 15 additive components.

The implementation of `FGAM` is available from the `refund` package in R (Goldsmith et al., 2020). The method fits a model of the form

$$F(X) = \mu + \int G(X(t), t)dt,$$

where $\mu \in \mathbb{R}$, and G is estimated using bivariate B-splines with roughness penalties. A restricted maximum likelihood approach is applied to select the parameter that penalizes the second order marginal differences of the basis (see the documentation of `fgam` in the `refund` package for details). We chose to use tensor-type bivariate cubic B-splines of dimensions 15 by 15. In all our settings, this choice ensured a stable fit and almost always resulted in the best performance compared to using other B-splines bases.

We implemented `TFBoost` in R, including `TFBoost(A.K)` for any positive integer K and `TFBoost(B)`. We fitted decision trees using the `rpart` package (Therneau and Atkinson, 2019) and performed optimization of `TFBoost(A.K)` using the `Nelder_Mead` function from the `lme4` package (Bates et al., 2015). The code implementing our method is publicly available online at <https://github.com/xmengju/TFBoost>. To make a fair comparison with its alternatives, we used cubic B-splines with 7 functions (3 evenly spaced interior knots) as the basis for `TFBoost` methods, same as what we did for `FLM1`, `FPPR`, and `FAME`. We then orthonormalized the basis as required by Type A and Type B trees.

We studied the performance of `TFBoost(A.K)` with $K = 1, 2$, and 3 ; and `TFBoost(B)` using 200 random directions at each iteration. For each of these methods, the maximum depth (d) of the functional multi-index trees was fixed for all iterations. We experimented with $d \in \{1, 2, 3, 4\}$ and for each method selected the value of d that achieved the lowest MSPE on the validation set at the early stopping time. We set the shrinkage parameter γ to 0.05 and the maximum number of iterations T_{\max} to 1000.

As mentioned in Section 2.1.1, the estimation of a Type A tree may result in a non-convex optimization problem. To avoid suboptimal local minima, we fitted each Type A

tree with multiple starting points. More specifically, we first uniformly sampled 30 points in the spherical coordinates system that satisfied the box constraints in (15) and ran the Nelder-Mead algorithm for 10 steps using each of the 30 points as the starting point. We then chose the five ending points with the lowest objective values and continued running the Nelder-Mead algorithm until convergence. Out of the five resulting estimates, we chose the one that minimized the objective function.

The results for all methods under consideration were evaluated in terms of the MSPE on the test set (\mathcal{T}):

$$\text{MSPE} = \frac{1}{|\mathcal{T}|} \sum_{i \in \mathcal{T}} (\hat{F}(x_i) - y_i)^2. \quad (21)$$

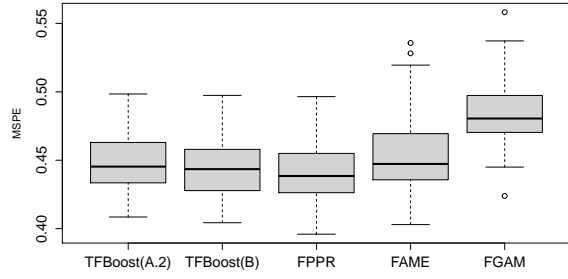
For **TFBoost**, the estimate \hat{F} was reported at the early stopping time.

3.2 Results

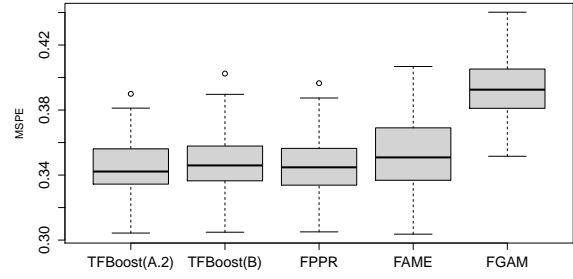
For each combination of the regression function (r_1, \dots, r_4) and the predictor model (M_1, M_2) , the results for the high noise (S_1) settings look very similar as those for the low noise (S_2) settings. In S_2 settings, the differences between estimators are more pronounced, showing a larger advantage of **TFBoost(A.K)** and **TFBoost(B)** over the others. We report here the results for S_1 settings and provide those for S_2 in the Appendix.

Figures 2 to 5 show the MSPEs on the test sets for r_1 to r_4 respectively. Since **FLM1**, **FLM2**, and **FAM** tend to produce very large errors, to be able to visualize the differences among the other methods, we excluded them from the figures and reported the summary statistics of their MSPEs in the Appendix. As expected, the linear estimators (**FLM1** and **FLM2**) do not work well since r_1 to r_4 are nonlinear functions. **FAM** also performs poorly, likely due to its using one FPC as the projection direction for each additive component, making it less flexible compared with estimating the projection direction based on the data.

In each figure, panel (a) corresponds to data with the predictors generated from M_1 and panel (b) for those from M_2 . Each panel shows the boxplot of MSPEs on the test sets from 100 independent runs of the experiment. For **TFBoost(A.K)**, we show the MSPEs for the value of K that gave the best results on the test sets, and include the rest in the Appendix. In the case of a tie we picked the simpler model (one with a smaller K). As a result, we selected

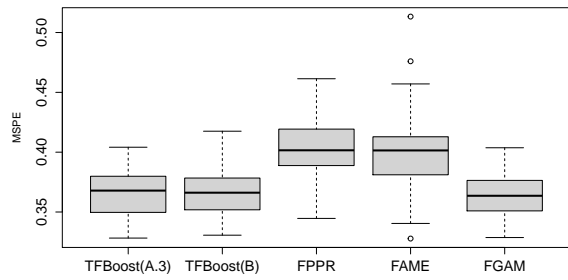


(a) M_1

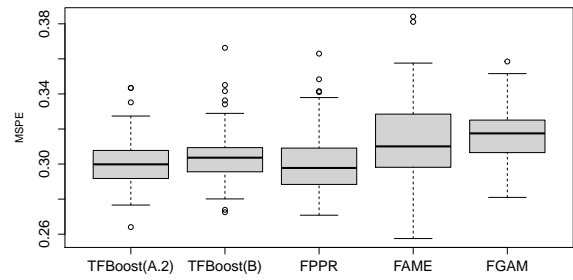


(b) M_2

Figure 2: Boxplots of MSPEs on test sets from 100 runs of the experiment with data generated from (r_1, M_1, S_1) in panel (a) and (r_1, M_2, S_1) in panel (b).

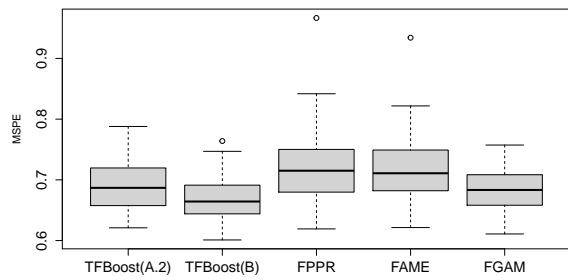


(a) M_1

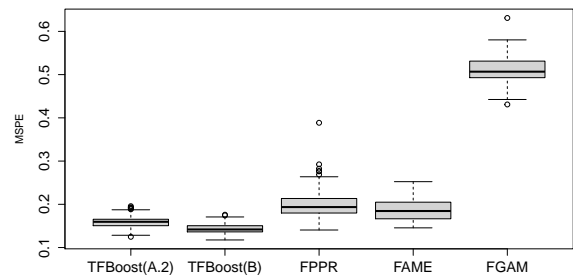


(b) M_2

Figure 3: Boxplots of MSPEs on test sets from 100 runs of the experiment with data generated from (r_2, M_1, S_1) in panel (a) and (r_2, M_2, S_1) in panel (b).



(a) M_1



(b) M_2

Figure 4: Boxplots of MSPEs on test sets from 100 runs of the experiment with data generated from (r_3, M_1, S_1) in panel (a) and (r_3, M_2, S_1) in panel (b).

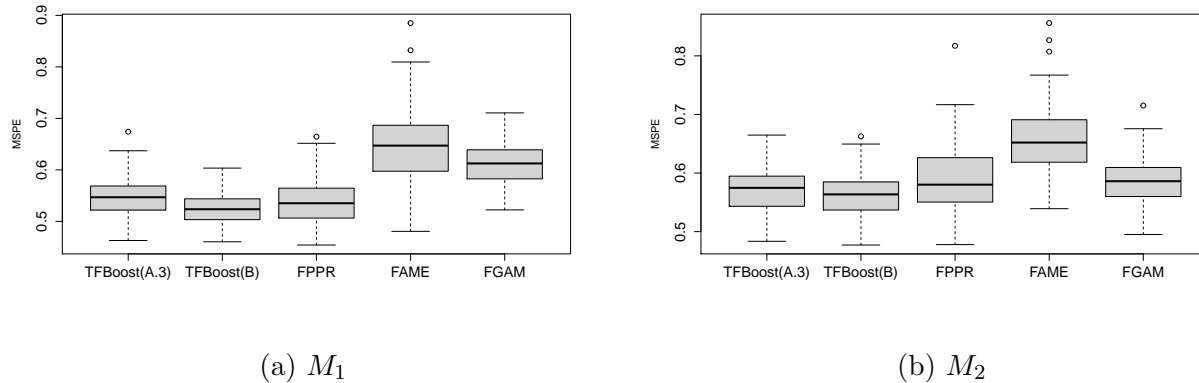


Figure 5: Boxplots of MSPEs on test sets from 100 runs of the experiment with data generated from (r_4, M_1, S_1) in panel (a) and (r_4, M_2, S_1) in panel (b).

- $K = 2$ for all r_1 and r_3 settings, and (r_2, M_2) ,
- $K = 3$ for all r_4 settings and (r_2, M_1) .

In general, **TFBoost(A.K)** and **TFBoost(B)** show stable and remarkable predictive performance in all these figures, with either or both achieving the lowest or second lowest average test MSPEs amongst all. In contrast, the performance of **FPPR**, **FAME**, and **FGAM** heavily depends on the regression function as well as the predictor model. For example, in panel (a) of Figure 3 where X was generated from M_1 , **FPPR** produces the worst errors compared to the other methods. However, when X followed M_2 in panel (b), **FPPR** becomes one of the best. The opposite holds for **FGAM**, being among the best in panel (a) and the worst in panel (b). Similarly in Figure 4, the performance of **FGAM** differs greatly in M_1 and M_2 settings. In Figures 2 and 5, the performances of **FAME** and **FGAM** are similar in both M_1 and M_2 settings, but they differ substantially across figures. **FGAM** produces significantly worse errors compared to **FAME** in Figure 2, whereas in Figure 5 we observe the opposite.

It is worth noting that **TFBoost** methods are close to their alternatives in terms of test errors when the true model matches the one on which the other methods are based. For example, in Figure 2 **TFBoost(A.2)** and **TFBoost(B)** produce similar errors as **FPPR**, where the regression function r_2 matches with the true model of **FPPR** specified with a single additive component. In other cases where the alternatives deviate from the true model, **TFBoost(A.K)** and **TFBoost(B)** usually show the lowest errors and their performances are

stable regardless of the setting. This illustrates the flexibility of our method, which helps to achieve low prediction errors without posing strong assumptions on the target function.

So far we have focused on the performance of **TFBoost** in nonlinear settings since the base learners are nonlinear. In the Appendix, we provide also results for an experiment fitting **TFBoost** methods with data generated from a linear model and comparing them with alternatives considered previously. As expected, the linear estimators **FLM1**, **FLM2** outperform the others. For **FGAM**, we note that the linear regression function matches with its model assumptions, which explains its good performance in linear settings. We note that the test errors of **TFBoost**(A.1) are only slightly worse than those produced by linear estimators: about 5% worse in the M_1 setting, and about 7% worse in the M_2 setting. This implies that even though **TFBoost** is an estimator for possibly nonlinear regression functions, we do not lose much applying it to data generated from linear models.

4 German electricity data

To illustrate the use of **TFBoost**, we analyzed a data set consisting of electricity spot prices traded at the European Energy Exchange (EEX) in Leipzig and electricity demand reported by the European Network of Transmission System Operators for Electricity from January 1st 2006 to September 30th 2008. On each day, electricity spot prices and demands were recorded hourly and represented as vectors of dimension 24. Our objective is to predict the daily average of electricity demand using hourly electricity spot prices. The whole dataset is available from the on-line supplementary materials of Liebl et al. (2013). To avoid days with known atypical price or demand values affecting our analysis, we removed weekends and holidays and analyzed data collected on the remaining 638 days. For each of these days, we view the hourly electricity spot prices as discretized evaluations of a smooth price function.

We considered methods of **TFBoost**(A,K) with $K = 1, 2, \text{ and } 3$, **TFBoost**(B), as well as their alternatives **FLM1**, **FLM2**, **FAM**, **FPPR**, **FAME**, and **FGAM**. To adjust for potential seasonality effects, we created a “day of the year” variable defined as the number of days from January 1st of the year in which the data were collected. In order to compare the results before and after adjusting for seasonality, our analysis consisted of two parts: (1) predicting daily

electricity demand with hourly electricity prices only, and (2) with both hourly electricity prices and the “day of the year” variable.

In part (1), all methods under consideration were specified in the same way as in Section 3.1. In part (2), we added “day of the year” as an additional predictor to all methods and adjusted their algorithms accordingly. For **TFBoost** methods, at every boosting iteration, we added “day of the year” as an additional variable to the functional multi-index tree. For the competitors, we included the scalar predictor in the model following the same approach as we did for the functional predictor. We added “day of the year” as a linear term in **FLM1** and **FLM2**, and as a nonparametric term in **FAM**, **FPPR**, **FAME**, and **FGAM**. For each of **FAM** and **FPPR**, we first calculated the estimator in the same way as in part (1) and obtained the residuals. Then we added to the part (1) estimator a Nadaraya-Watson estimator with Gaussian kernel fitted to the residuals using “day of the year” as the predictor. For **FAME** and **FGAM** we specified a smooth term on “day of the year” represented as penalized cubic splines (Wood, 2017). Other than adding this additional predictor, the other parameters and fitting procedures were kept the same as in part (1).

We randomly partitioned the data into a training set (60%), a validation set (20%), and a test set (20%). As in Section 3, we fitted each model using the training and validation sets and recorded MSPE on the test set. The validation set was used to choose the regularization parameter of **FLM1**, the number of additive components of **FAM** and **FPPR**, and the maximum tree depth and early stopping time of **TFBoost(A,1)**, **TFBoost(A,2)**, **TFBoost(A,3)**, and **TFBoost(B)**.

To reduce the variability introduced by partitioning the data, we repeated the experiment with 100 random data splits. Figures 6 and 7 show test MSPEs obtained from 100 random data splits in part (1) and (2) of the experiment respectively. The summary statistics of these test MSPEs are provided in the Appendix. To better reveal the differences between the estimators under consideration, in each figure the y-axis is truncated and represents test MSPE $\times 10^{-6}$.

In both figures, **TFBoost(A.1)**, **TFBoost(A.2)**, **TFBoost(A.3)**, and **TFBoost(B)** show superior performance compared to their alternatives. They achieve the lowest errors with the smallest standard errors. In Figure 6, we observe that **TFboost(B)** produces the smallest test errors, substantially better than **FLM1**, **FLM2**, **FAM**, and **FGAM**. The performance of

FPPR is the closest to TFBoost(B), however, it is much more expensive to fit kernel estimators compared to Type B trees, particularly with data of a large sample size. Comparing Figure 7 with Figure 6, we observe improvements in test errors for all methods except for FLM1. This implies the importance of adjusting for seasonality when predicting the electricity demand, which is likely due to higher electricity usage in the summer for cooling and in the winter for heating. In Figure 7, TFBoost(A.1), TFBoost(A.2), TFBoost(A.3) produce very similar results, and TFBoost(A.2) outperforms the other two by a small margin in terms of the average test MSPE.

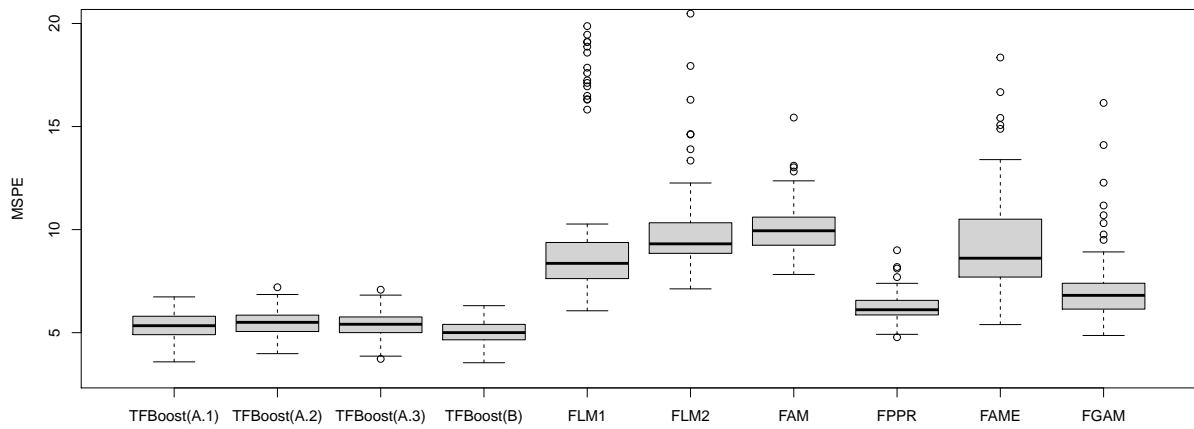


Figure 6: Boxplot of test MSPEs obtained from 100 random splits of the data from part (1) of the experiment. The unit of y-axis is 10^{-6} .

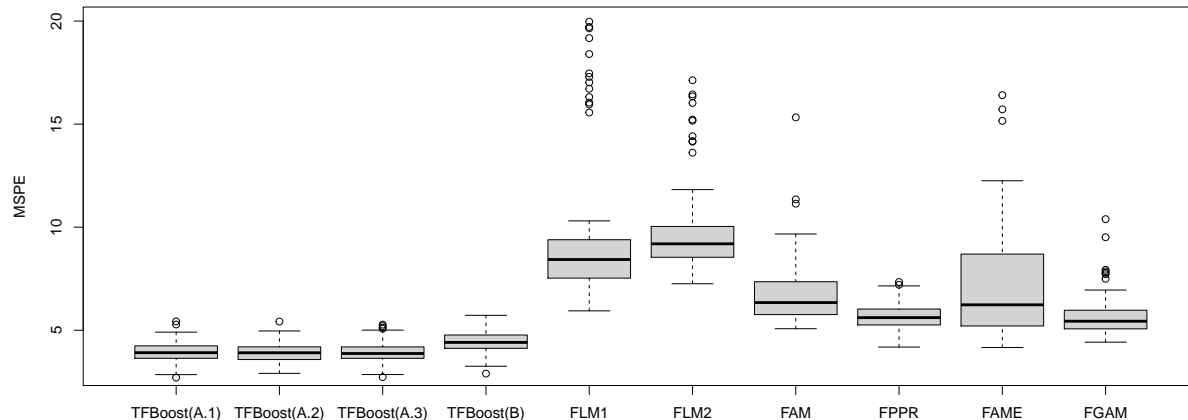


Figure 7: Boxplot of test MSPEs obtained from 100 random splits of the data from part (2) of the experiment. The unit of y-axis is 10^{-6} .

5 Conclusion and future work

In this paper we have proposed a novel boosting method for regression with a functional explanatory variable. Our approach uses functional multi-index trees as base learners, which offer flexibility and are relatively easy to fit. Compared with widely studied single index estimators, our multi-index estimator enables modelling possible interactions between indices, allowing us to better approximate complex regression functions. Through extensive numerical experiments, we demonstrate that our method consistently produces one of the lowest prediction errors across different settings, while available alternatives can be seriously affected by model misspecification. In addition, **TFBoost** with Type B learners exhibits significant computational advantages over kernel-based methods, being able to provide accurate predictions at a much lower cost.

The methodology of **TFBoost** suggests a number of interesting areas for future work. First, we formulated the regression problem with a single functional predictor, but in principle, it could also be extended to multiple predictors, functional or scalar. This can be achieved by including indices calculated from multiple predictors, either allowing each index to be associated with all predictors or one of the predictors. If there are many predictors, this approach may be computationally difficult and can result in unstable estimators when

the sample size is small. In this situation, we need to assume sparsity in the functional space, which means that some but not all predictors are related to the response. Group penalties with projections on each predictor being a group can be considered to enable variable selection. Second, in our experiments we only studied `TFBoost` applied with the squared loss. In cases where data contain outliers, it will be useful to consider fitting our method with different loss functions, for example, Huber's or Tukey's loss. Finally, in this paper we focused on functional predictors observed at many time points without measurement errors. In practice, one may encounter situations where only very few and possibly noisy measurements of the predictor function are available. In this case, smoothing each predictor curve provides unreliable approximations and makes them poor inputs to `TFBoost`. It may be more advisable to borrow strength across curves, for example, fitting `TFBoost` to curves reconstructed using FPCA (Yao et al. (2005) and Boente and Salibián-Barrera (2021)).

6 Acknowledgments

The authors gratefully thank Professor James and Professor Ferraty for sharing the code used in their papers (James and Silverman (2005) and Ferraty et al. (2013)). This research was supported by the Natural Sciences and Engineering Research Council of Canada [Discovery Grant RGPIN-2016-04288].

APPENDICES

Appendix A

Proof of Theorem 1 in Section 2.1.1.

Proof 1 *It is clear that if $\{\beta_1, \dots, \beta_K\} = \{(-1)^{l_1}\eta_1, \dots, (-1)^{l_K}\eta_K\}$ for some $l_1, \dots, l_K \in \{0, 1\}$, then $g = \tilde{g}$. Therefore, it suffices to show that $\{\beta_1, \dots, \beta_K\} = \{(-1)^{l_1}\eta_1, \dots, (-1)^{l_K}\eta_K\}$ for some $l_1, \dots, l_K \in \{0, 1\}$. We prove that if there do not exist l_1, \dots, l_K for the two sets to be equal, there exists a set of indices for which (12) is a constant function and thus contradicts Condition 2.*

For simplicity, we let $\tilde{\eta}_j = (-1)^{l_j}\eta_j$. If for any l_1, \dots, l_K $\{\beta_1, \dots, \beta_K\} \neq \{\tilde{\eta}_1, \dots, \tilde{\eta}_K\}$, we match two sets so that the same vectors β_j and $\tilde{\eta}_j$ align with each other. We let $S = \{\beta_1, \dots, \beta_K\} \cap \{\tilde{\eta}_1, \dots, \tilde{\eta}_K\}$, $\beta_j = \tilde{\eta}_j$, for $j = 1, \dots, |S|$ and $\beta_j \notin \{\tilde{\eta}_1, \dots, \tilde{\eta}_K\}$, for $j = |S| + 1, \dots, K$, and $|S| < K$. By Condition 2, there exist a x_0 for $J = |S| + 1, \dots, K$, (12) is not a constant function.

By (13), Condition 1 and Condition 2, for any $t_1, \dots, t_K \in (-\delta, \delta)$

$$\begin{aligned} h(\langle x_0, \beta_1 \rangle + t_1, \dots, \langle x_0, \beta_K \rangle + t_K) &= h(\langle x_0 + t_1\beta_1, \beta_1 \rangle, \dots, \langle x_0 + t_K\beta_K, \beta_K \rangle) \\ &= \tilde{h}(\langle x_0 + t_1\beta_1, \eta_1 \rangle, \dots, \langle x_0 + t_K\beta_K, \eta_K \rangle) \\ &= \tilde{h}(\langle x_0, \eta_1 \rangle + t_1\langle \beta_1, \eta_1 \rangle, \dots, \langle x_0, \eta_K \rangle + t_K\langle \beta_K, \eta_K \rangle) \end{aligned}$$

and similarly

$$\begin{aligned} \tilde{h}(\langle x_0, \eta_1 \rangle + t_1, \dots, \langle x_0, \eta_K \rangle + t_K) &= \tilde{h}(\langle x_0 + t_1\eta_1, \eta_1 \rangle, \dots, \langle x_0 + t_K\eta_K, \eta_K \rangle) \\ &= h(\langle x_0 + t_1\eta_1, \beta_1 \rangle, \dots, \langle x_0 + t_K\eta_K, \beta_K \rangle) \\ &= h(\langle x_0, \beta_1 \rangle + t_1\langle \beta_1, \eta_1 \rangle, \dots, \langle x_0, \beta_K \rangle + t_K\langle \beta_K, \eta_K \rangle) \end{aligned}$$

By Cauchy-Schwarz inequality and Condition 1, $(\langle \beta_j, \eta_j \rangle)^2 = 1$ for $j = 1, \dots, |S|$ and

$(\langle \beta_j, \eta_j \rangle)^2 < 1$ for $j = |S + 1|, \dots, K$. For any $t_1, \dots, t_K \in (-\delta, \delta)$,

$$\begin{aligned}
h(\langle x_0, \beta_1 \rangle + t_1, \dots, \langle x_0, \beta_K \rangle + t_K) &= \tilde{h}(\langle x_0, \eta_1 \rangle + t_1 \langle \beta_1, \eta_1 \rangle, \dots, \langle x_0, \eta_K \rangle + t_K \langle \beta_K, \eta_K \rangle) \\
&= h(\langle x_0, \beta_1 \rangle + t_1 \langle \beta_1, \eta_1 \rangle^2, \dots, \langle x_0, \beta_K \rangle + t_K \langle \beta_K, \eta_K \rangle^2) \\
&\vdots \\
&= h(\langle x_0, \beta_1 \rangle + t_1 \langle \beta_1, \eta_1 \rangle^{2n}, \dots, \langle x_0, \beta_K \rangle + t_K \langle \beta_K, \eta_K \rangle^{2n}) \\
&\vdots \\
&= h(\langle x_0, \beta_1 \rangle + t_1 I_1, \dots, \langle x_0, \beta_K \rangle + t_K I_K) \tag{22}
\end{aligned}$$

where $I_j = 1$ for $j = 1, \dots, |S|$ and $I_j = 0$ for $j = |S + 1|, \dots, |K|$.

Let $x = x_0 + te$ for any unit function $e \in L^2(\mathcal{I})$, $\|e\| = 1$ and $t \in (-\delta, \delta)$. Then x fills the space of $B(x_0, \delta)$. For $j = 1, \dots, K$, we define

$$\begin{aligned}
L_j(x) &= (1 - I_j)x + I_j x_0 \\
&= (1 - I_j)(x_0 + te) + I_j x_0 \\
&= x_0 + (1 - I_j)te
\end{aligned}$$

$$\begin{aligned}
h(\langle L_1(x), \beta_1 \rangle, \dots, \langle L_K(x), \beta_K \rangle) &= h(\langle x_0 + (1 - I_1)te, \beta_1 \rangle, \dots, \langle x_0 + (1 - I_K)te, \beta_K \rangle) \\
&= h(\langle x_0, \beta_1 \rangle + \langle (1 - I_1)te, \beta_1 \rangle, \dots, \langle x_0, \beta_K \rangle + \langle (1 - I_K)te, \beta_K \rangle), \text{ by (22)} \\
&= h(\langle x_0, \beta_1 \rangle + \langle I_1(1 - I_1)te, \beta_1 \rangle, \dots, \langle x_0, \beta_K \rangle + \langle I_K(1 - I_K)te, \beta_K \rangle) \\
&= h(\langle x_0, \beta_1 \rangle, \dots, \langle x_0, \beta_K \rangle),
\end{aligned}$$

which is a constant function of x and that contradicts Condition 2.

Appendix B

The summary statistics of test MSPEs from 100 independent runs of the simulation are included below, with bold font indicating the lowest two average test errors in each setting.

	SNR = 20		SNR = 5	
	M_1	M_2	M_1	M_2
TFBoost(A.1)	0.118 (0.006)	0.090 (0.004)	0.449 (0.022)	0.347 (0.016)
TFBoost(A.2)	0.118 (0.006)	0.090 (0.004)	0.448 (0.020)	0.345 (0.016)
TFBoost(A.3)	0.120 (0.006)	0.090 (0.004)	0.451 (0.021)	0.346 (0.016)
TFBoost(B)	0.116 (0.005)	0.091 (0.004)	0.444 (0.021)	0.346 (0.016)
FLM1	0.218 (0.009)	0.223 (0.009)	0.534 (0.022)	0.537 (0.023)
FLM2	0.219 (0.008)	0.200 (0.008)	0.535 (0.021)	0.446 (0.019)
FAM	0.270 (0.044)	0.189 (0.009)	0.590 (0.055)	0.435 (0.020)
FPPR	0.113 (0.006)	0.089 (0.005)	0.440 (0.021)	0.347 (0.018)
FAME	0.117 (0.007)	0.094 (0.007)	0.454 (0.028)	0.352 (0.021)
FGAM	0.150 (0.008)	0.134 (0.007)	0.484 (0.023)	0.393 (0.018)

Table 1: Summary statistics of test errors for data generated from r_1 ; displayed in the form of mean (sd).

	SNR = 20		SNR = 5	
	M_1	M_2	M_1	M_2
TFBoost(A.1)	0.143 (0.009)	0.091 (0.005)	0.372 (0.019)	0.303 (0.014)
TFBoost(A.2)	0.134 (0.009)	0.089 (0.005)	0.366 (0.018)	0.300 (0.014)
TFBoost(A.3)	0.130 (0.009)	0.089 (0.005)	0.365 (0.018)	0.300 (0.014)
TFBoost(B)	0.124 (0.008)	0.091 (0.005)	0.366 (0.019)	0.304 (0.015)
FLM1	0.610 (0.032)	0.177 (0.011)	0.815 (0.040)	0.376 (0.018)
FLM2	0.611 (0.032)	0.176 (0.011)	0.817 (0.041)	0.376 (0.017)
FAM	0.303 (0.044)	0.138 (0.013)	0.510 (0.047)	0.339 (0.019)
FPPR	0.155 (0.014)	0.092 (0.008)	0.402 (0.024)	0.301 (0.017)
FAME	0.147 (0.013)	0.099 (0.010)	0.399 (0.030)	0.314 (0.021)
FGAM	0.148 (0.009)	0.113 (0.008)	0.364 (0.018)	0.316 (0.014)

Table 2: Summary statistics of test errors for data generated from r_2 ; displayed in the form of mean (sd).

	SNR = 20		SNR = 5	
	M_1	M_2	M_1	M_2
TFBoost(A.1)	0.220 (0.016)	0.082 (0.013)	0.694 (0.037)	0.161 (0.015)
TFBoost(A.2)	0.217 (0.014)	0.079 (0.012)	0.690 (0.038)	0.159 (0.014)
TFBoost(A.3)	0.213 (0.014)	0.080 (0.011)	0.690 (0.037)	0.160 (0.014)
TFBoost(B)	0.195 (0.011)	0.061 (0.009)	0.669 (0.035)	0.143 (0.011)
FLM1	1.358 (0.061)	0.804 (0.041)	1.788 (0.086)	1.223 (0.054)
FLM2	1.354 (0.064)	0.689 (0.038)	1.785 (0.087)	0.758 (0.039)
FAM	0.879 (0.092)	0.501 (0.043)	1.312 (0.103)	0.571 (0.044)
FPPR	0.237 (0.028)	0.114 (0.033)	0.718 (0.056)	0.202 (0.037)
FAME	0.228 (0.019)	0.094 (0.023)	0.719 (0.053)	0.186 (0.025)
FGAM	0.219 (0.013)	0.438 (0.029)	0.683 (0.036)	0.511 (0.031)

Table 3: Summary statistics of test errors for data generated from r_3 ; displayed in the form of mean (sd).

	SNR = 20		SNR = 5	
	M_1	M_2	M_1	M_2
TFBoost(A.1)	0.253 (0.020)	0.271 (0.027)	0.571 (0.038)	0.582 (0.037)
TFBoost(A.2)	0.236 (0.018)	0.262 (0.024)	0.557 (0.034)	0.575 (0.036)
TFBoost(A.3)	0.226 (0.019)	0.259 (0.026)	0.547 (0.035)	0.572 (0.037)
TFBoost(B)	0.196 (0.017)	0.247 (0.026)	0.524 (0.030)	0.563 (0.038)
FLM1	1.438 (0.071)	0.586 (0.036)	1.712 (0.080)	0.857 (0.047)
FLM2	1.455 (0.071)	0.586 (0.036)	1.727 (0.080)	0.855 (0.045)
FAM	0.902 (0.144)	0.526 (0.041)	1.179 (0.148)	0.797 (0.051)
FPPR	0.209 (0.024)	0.265 (0.052)	0.540 (0.048)	0.589 (0.058)
FAME	0.324 (0.058)	0.346 (0.051)	0.651 (0.071)	0.656 (0.059)
FGAM	0.300 (0.027)	0.290 (0.032)	0.611 (0.038)	0.588 (0.042)

Table 4: Summary statistics of test errors for data generated from r_4 ; displayed in the form of mean (sd).

Appendix C

We consider another regression function that is linear:

$$r_5(X) = \int_{\mathcal{I}} \left(\sin\left(\frac{3}{2}\pi t\right) + \sin\left(\frac{1}{2}\pi t\right) \right) X(t) dt.$$

The other specifications of the model remain the same as described in Section 3. Table 5 includes the summary statistics of test MSPEs from 100 independent runs of the simulation, with bold font indicating the lowest two average test errors in each setting.

	SNR = 20		SNR = 5	
	M_1	M_2	M_1	M_2
TFBoost(A.1)	0.106 (0.005)	0.035 (0.002)	0.415 (0.019)	0.132 (0.006)
TFBoost(A.2)	0.107 (0.005)	0.035 (0.002)	0.419 (0.019)	0.134 (0.006)
TFBoost(A.3)	0.108 (0.005)	0.035 (0.002)	0.418 (0.020)	0.134 (0.006)
TFBoost(B)	0.109 (0.005)	0.037 (0.002)	0.420 (0.020)	0.136 (0.006)
FLM1	0.100 (0.005)	0.031 (0.001)	0.398 (0.018)	0.124 (0.006)
FLM2	0.099 (0.004)	0.031 (0.001)	0.396 (0.018)	0.123 (0.005)
FAM	0.146 (0.028)	0.033 (0.002)	0.442 (0.037)	0.125 (0.006)
FPPR	0.102 (0.005)	0.036 (0.010)	0.407 (0.022)	0.129 (0.009)
FAME	0.102 (0.005)	0.032 (0.002)	0.407 (0.023)	0.127 (0.008)
FGAM	0.099 (0.004)	0.031 (0.001)	0.396 (0.017)	0.123 (0.005)

Table 5: Summary statistics of test errors for data generated from r_5 ; displayed in the form of mean (sd).

Appendix D

The summary statistics of test MSPEs from 100 random partitions of the German electricity data in Section 4 are provided below.

	Part (1)	Part (2)
TFBoost(A.1)	5.333 (0.633)	3.880 (0.480)
TFBoost(A.2)	5.370 (0.627)	3.828 (0.446)
TFBoost(A.3)	5.259 (0.615)	3.887 (0.472)
TFBoost(B)	4.903 (0.568)	4.353 (0.513)
FLM1	10.614 (4.851)	10.679 (5.068)
FLM2	13.040 (11.654)	11.487 (6.058)
FAM	12.667 (16.582)	9.476 (17.453)
FPPR	6.235 (0.716)	5.721 (0.704)
FAME	13.888 (15.054)	8.581 (6.617)
FGAM	7.406 (2.202)	5.756 (1.050)

Table 6: Summary statistics of test MSPEs displayed in the form of mean (sd). The unit of MSPEs is 10^{-6} .

References

- Ait-Saïdi, A., Ferraty, F., Kassa, R., and Vieu, P. (2008). Cross-validated estimations in the single-functional index model. *Statistics*, 42(6):475–494.
- Amato, U., Antoniadis, A., and De Feis, I. (2006). Dimension reduction in functional regression with applications. *Computational Statistics & Data Analysis*, 50(9):2422–2446.
- Amiri, A., Crambes, C., and Thiam, B. (2014). Recursive estimation of nonparametric regression with functional covariate. *Computational Statistics & Data Analysis*, 69:154–172.
- Avery, M., Wu, Y., Helen Zhang, H., and Zhang, J. (2014). RKHS-based functional non-parametric regression for sparse and irregular longitudinal data. *Canadian Journal of Statistics*, 42(2):204–216.
- Baïllo, A. and Grané, A. (2009). Local linear regression for functional predictor and scalar response. *Journal of Multivariate Analysis*, 100(1):102–111.

- Barrientos-Marin, J., Ferraty, F., and Vieu, P. (2010). Locally modelled regression and functional data. *Journal of Nonparametric Statistics*, 22(5):617–632.
- Bates, D., Mächler, M., Bolker, B., and Walker, S. (2015). Fitting linear mixed-effects models using lme4. *Journal of Statistical Software*, 67(1):1–48.
- Berlinet, A., Elamine, A., and Mas, A. (2011). Local linear regression for functional data. *Annals of the Institute of Statistical Mathematics*, 63(5):1047–1075.
- Blumenson, L. (1960). A derivation of n-dimensional spherical coordinates. *The American Mathematical Monthly*, 67(1):63–66.
- Boente, G. and Salibian-Barrera, M. (2021). Robust functional principal components for sparse longitudinal data. *METRON*, 79(2):1–30.
- Breiman, L., F. J. O. R. . S. C. (1984). *Classification And Regression Trees (1st ed.)*. Routledge.
- Burba, F., Ferraty, F., and Vieu, P. (2009). K-nearest neighbour method in functional nonparametric regression. *Journal of Nonparametric Statistics*, 21(4):453–469.
- Cardot, H., Ferraty, F., and Sarda, P. (1999). Functional linear model. *Statistics & Probability Letters*, 45(1):11–22.
- Cardot, H., Ferraty, F., and Sarda, P. (2003). Spline estimators for the functional linear model. *Statistica Sinica*, 13(3):571–591.
- Cardot, H. and Sarda, P. (2005). Estimation in generalized linear models for functional data via penalized likelihood. *Journal of Multivariate Analysis*, 92(1):24–41.
- Carroll, C., Gajardo, A., Chen, Y., Dai, X., Fan, J., Hadjipantelis, P. Z., Han, K., Ji, H., Mueller, H.-G., and Wang, J.-L. (2021). *fdapace: Functional Data Analysis and Empirical Dynamics*. R package version 0.5.6.
- Chen, D., Hall, P., Müller, H.-G., et al. (2011). Single and multiple index functional regression models with nonparametric link. *The Annals of Statistics*, 39(3):1720–1747.

- Dou, W. W., Pollard, D., Zhou, H. H., et al. (2012). Estimation in functional regression for general exponential families. *The Annals of Statistics*, 40(5):2421–2451.
- Fan, Y., James, G. M., Radchenko, P., et al. (2015). Functional additive regression. *The Annals of Statistics*, 43(5):2296–2325.
- Febrero-Bande, M. and González-Manteiga, W. (2013). Generalized additive models for functional data. *Test*, 22(2):278–292.
- Ferraty, F., Goia, A., Salinelli, E., and Vieu, P. (2013). Functional projection pursuit regression. *Test*, 22(2):293–320.
- Ferraty, F., Hall, P., and Vieu, P. (2010). Most-predictive design points for functional data predictors. *Biometrika*, 97(4):807–824.
- Ferraty, F., Park, J., and Vieu, P. (2011). Estimation of a functional single index model. In Ferraty, F., editor, *Recent Advances in Functional Data Analysis and Related Topics*, Contributions to Statistics, Heidelberg. Physica-Verlag HD.
- Ferraty, F., Peuch, A., and Vieu, P. (2003). Modèle à indice fonctionnel simple. *Comptes Rendus Mathématique*, 336(12):1025–1028.
- Ferraty, F. and Vieu, P. (2002). The functional nonparametric model and application to spectrometric data. *Computational Statistics*, 17(4):545–564.
- Ferraty, F. and Vieu, P. (2006). *Nonparametric functional data analysis: theory and practice*. Springer, New York, NY.
- Ferraty, F. and Vieu, P. (2009). Additive prediction and boosting for functional data. *Computational Statistics & Data Analysis*, 53(4):1400–1413.
- Ferré, L. and Yao, A.-F. (2003). Functional sliced inverse regression analysis. *Statistics*, 37(6):475–488.
- Friedman, J. H. (2001). Greedy function approximation: a gradient boosting machine. *Annals of statistics*, 29(5):1189–1232.

- Geenens, G. et al. (2011). Curse of dimensionality and related issues in nonparametric functional regression. *Statistics Surveys*, 5:30–43.
- Goia, A. and Vieu, P. (2015). A partitioned single functional index model. *Computational Statistics*, 30(3):673–692.
- Goldsmith, J., Scheipl, F., Huang, L., Wrobel, J., Di, C., Gellar, J., Harezlak, J., McLean, M. W., Swihart, B., Xiao, L., Crainiceanu, C., and Reiss, P. T. (2020). *refund: Regression with Functional Data*. R package version 0.1-23.
- Greven, S. and Scheipl, F. (2017). A general framework for functional regression modelling. *Statistical Modelling*, 17(1-2):1–35.
- Hall, P., Horowitz, J. L., et al. (2007). Methodology and convergence rates for functional linear regression. *The Annals of Statistics*, 35(1):70–91.
- Hastie, T. and Mallows, C. (1993). A statistical view of some chemometrics regression tools. *Technometrics*, 35(2):140–143.
- James, G. M. (2002). Generalized linear models with functional predictors. *Journal of the Royal Statistical Society: Series B (Statistical Methodology)*, 64(3):411–432.
- James, G. M. and Silverman, B. W. (2005). Functional adaptive model estimation. *Journal of the American Statistical Association*, 100(470):565–576.
- Jiang, C.-R., Wang, J.-L., et al. (2011). Functional single index models for longitudinal data. *The Annals of Statistics*, 39(1):362–388.
- Kara, L.-Z., Laksaci, A., Rachdi, M., and Vieu, P. (2017). Data-driven KNN estimation in nonparametric functional data analysis. *Journal of Multivariate Analysis*, 153:176–188.
- Kudraszow, N. L. and Vieu, P. (2013). Uniform consistency of knn regressors for functional variables. *Statistics & Probability Letters*, 83(8):1863–1870.
- Li, K.-C. (1991). Sliced inverse regression for dimension reduction. *Journal of the American Statistical Association*, 86(414):316–327.

- Lian, H. and Li, G. (2014). Series expansion for functional sufficient dimension reduction. *Journal of Multivariate Analysis*, 124:150–165.
- Liebl, D. et al. (2013). Modeling and forecasting electricity spot prices: A functional data perspective. *The Annals of Applied Statistics*, 7(3):1562–1592.
- Ling, N. and Vieu, P. (2018). Nonparametric modelling for functional data: selected survey and tracks for future. *Statistics*, 52(4):934–949.
- Ling, N. and Vieu, P. (2020). On semiparametric regression in functional data analysis. *Wiley Interdisciplinary Reviews: Computational Statistics*, e1538. <https://doi.org/10.1002/wics.1538>.
- Mas, A. et al. (2012). Lower bound in regression for functional data by representation of small ball probabilities. *Electronic Journal of Statistics*, 6:1745–1778.
- McLean, M. W., Hooker, G., Staicu, A.-M., Scheipl, F., and Ruppert, D. (2014). Functional generalized additive models. *Journal of Computational and Graphical Statistics*, 23(1):249–269.
- Müller, H.-G., Stadtmüller, U., et al. (2005). Generalized functional linear models. *The Annals of Statistics*, 33(2):774–805.
- Müller, H.-G., Wu, Y., and Yao, F. (2013). Continuously additive models for nonlinear functional regression. *Biometrika*, 100(3):607–622.
- Müller, H.-G. and Yao, F. (2008). Functional additive models. *Journal of the American Statistical Association*, 103(484):1534–1544.
- Preda, C. (2007). Regression models for functional data by reproducing kernel hilbert spaces methods. *Journal of Statistical Planning and Inference*, 137(3):829–840.
- Reiss, P. T. and Ogden, R. T. (2007). Functional principal component regression and functional partial least squares. *Journal of the American Statistical Association*, 102(479):984–996.

- Shang, H. L. (2016). A Bayesian approach for determining the optimal semi-metric and bandwidth in scalar-on-function quantile regression with unknown error density and dependent functional data. *Journal of Multivariate Analysis*, 146:95–104.
- Telgarsky, M. (2013). Margins, shrinkage, and boosting. *International Conference on Machine Learning*, 28(2):307–315.
- Therneau, T. and Atkinson, B. (2019). *rpart: Recursive Partitioning and Regression Trees*. R package version 4.1-15.
- Tutz, G. and Gertheiss, J. (2010). Feature extraction in signal regression: a boosting technique for functional data regression. *Journal of Computational and Graphical Statistics*, 19(1):154–174.
- Wang, G., Lin, N., and Zhang, B. (2014). Functional K-means inverse regression. *Computational Statistics & Data Analysis*, 70:172–182.
- Wood, S. N. (2017). *Generalized additive models: an introduction with R (2nd ed.)*. Chapman and Hall/CRC.
- Yao, F., Müller, H.-G., and Wang, J.-L. (2005). Functional data analysis for sparse longitudinal data. *Journal of the American Statistical Association*, 100(470):577–590.
- Zhao, Y., Ogden, R. T., and Reiss, P. T. (2012). Wavelet-based lasso in functional linear regression. *Journal of Computational and Graphical Statistics*, 21(3):600–617.